IEEE Access
Multidisciplinary | Rapid Review | Open Access Journal

Received May 4, 2022, accepted May 21, 2022, date of publication May 25, 2022, date of current version June 1, 2022.

Digital Object Identifier 10.1109/ACCESS.2022.3177751

Assessment of the Influence of Hydrogen Share on Performance, Combustion, and Emissions in a Four-Stroke Gasoline Engine

MD. NURUN NABI[1], WISAM K. HUSSAM[2], MOHAMMAD TOWHIDUL ISLAM[3], AND S. M. MUYEEN[4], (Senior Member, IEEE)

[1]School of Engineering and Technology, Central Queensland University, Perth, WA 6000, Australia
[2]School of Engineering, Australian University, Safat 13015, Kuwait
[3]Department of Mechanical Engineering, Georgia Southern University, Statesboro, GA 30460, USA
[4]Department of Electrical Engineering, Qatar University, Doha, Qatar

Corresponding author: S. M. Muyeen (sm.muyeen@qu.edu.qa)

This research work was supported in part by the Kuwait Foundation for the Advancement of Sciences, Kuwait, under Grant CR19-45EM-01; in part by Central Queensland University, Australia, under Grant RSH/5221. The publication of this article was funded by Qatar National Library.

ABSTRACT This study aims to develop a one-dimensional model to investigate the effect of hydrogen share in gasoline fuel on the performance, combustion, and exhaust emissions of a gasoline direct-injection engine. Iso-octane was used as a reference fuel to compare performance, combustion, and emission parameters. The model was developed using commercial GT-Suite and ANSYS software. The simulation results using GT-Suite were validated with the published data and ANSYS results. The hydrogen fractions were varied from 0% to 11.09% to validate the simulation results with the published results. The investigation continued with three higher hydrogen fractions (15%, 20% and 25%) to study the performance, combustion, emissions, and sustainability parameters. Compared to neat gasoline, hydrogen-shared fuels show a maximum 2% higher exergy efficiency, 51% higher exergy and 42% energy rates while reducing carbon dioxide (CO_2) emissions by 51% with a penalty of nitrogen oxide emissions (NOx) by 62% at an excess ratio of 1.3. Other novel findings, including higher sustainability indices, lower depletion potentials, and lower unitary cost indices with higher-fraction hydrogen fuels, suggest that they are environmentally and economically sustainable. In the second part of this study, the NOx formation mechanism and its associated factors, including in-cylinder temperature, heat transfer rate, cumulative heat release, and burned rate, were confirmed and compared with gasoline and neat ethylene.

INDEX TERMS Hydrogen fuel, gasoline direct injection engine, performance, combustion, exhaust emissions.

I. INTRODUCTION

Anthropogenic activities, such as using petroleum fuels in transportation, contribute to harmful environmental emissions, and according to the literature, the transportation and industrial sectors are the largest consumers of fossil fuels [1]. Environmental and human health consequences compel researchers to develop fossil-based fuels and resources [2]. Concerning fuel consumption and exhaust emissions, hydrogen with a specific standard appears to be the most promising, cutting conventional diesel engines' fuel consumption and hazardous emissions dramatically [3]. Compared to 1990, European emission targets a 60% greenhouse gas emission reduction by 2050 and a 20% reduction by 2030 relative to 2008 [4]. Hydrogen is considered an alternative fuel for internal combustion engines due to its higher flame velocity and higher calorific value [5]. Hydrogen was also tested in a compression ignition engine to control the CO_2, and other criteria pollutants, including PM, THC and CO emissions. Nag *et al.* [6] conducted experiments with hydrogen fuel in a hydrogen-diesel dual-fuel engine. The experiment varied the engine load from 25% to 75% of the full load. Hydrogen energy was varied 0% to 20% (0%, 5%, 10% and 20%). They reported that sharing hydrogen energy with diesel

The associate editor coordinating the review of this manuscript and approving it for publication was Agustin Leobardo Herrera-May.

This work is licensed under a Creative Commons Attribution 4.0 License. For more information, see https://creativecommons.org/licenses/by/4.0/

improves the peak pressure and reduces engine knock at lower loads. Engine vibrations were increased at higher loads but were moderate at lower loads. However, the authors did not report any hydrogen-diesel dual fuel emissions or engine performance. Cernat *et al.* [7] conducted an experimental investigation with hydrogen as fuel in a K9K automotive diesel engine. They performed the experiments at an engine speed of 2000 rpm with 40%, 55%, 70% and 85% engine load and with different proportions of hydrogen. The authors reported a higher thermal efficiency and lower exhaust emissions, including CO_2, unburned hydrocarbon (HC), NOx and smoke emissions with the use of hydrogen as a fuel for compression ignition engines. Another study [8] investigated hydrogen introduction into an intake manifold of a diesel engine. The authors conducted similar experiments at engine speeds of 750 rpm, 900 rpm, 1100 rpm, 1400 rpm, 1750 rpm, and 2100 rpm with full load conditions. The authors reported a slight increase in HC emissions with a substantial reduction in CO_2 and carbon monoxide (CO) emissions with increased hydrogen fractions. The authors also reported an increased peak cylinder pressure and heat release rate with increased hydrogen fractions. Du *et al.* [9] did engine experiments with several hydrogen fractions (0%, 3.99%, 5.87%, 9.41%, and 11.09%) in a modified spark-ignition engine facilitated to hydrogen direct injection system. The experiments were performed at excess air ratios of 1.0, 1.1, 1.2, 1.3, 1.4 and 1.5. Their results informed improved mean effective pressure and thermal efficiency with the increase in hydrogen fractions. The authors also reported a decrease in CO and HC emissions with a penalty of NOx emissions. However, their study was limited to 11.09% hydrogen fractions. Martin *et al.* [10] experiment with a hybrid hydrogen-gasoline engine. The authors compared engine performance and exhaust emission results between reformed exhaust gas recirculation (rEGR) and traditional exhaust gas recirculation (EGR). The findings show that rEGR has the potential to improve thermal efficiency while lowering gaseous emissions and lowering PM generation all at the same time. However, their results did not include exergy and sustainability-related parameters. Like gasoline, ethylene could be used as a substitute fuel for a spark-ignition engine. Wan *et al.* [11] used a stainless steel shock tube to examine Ethylene-Air ignition behaviours at different temperatures. They found that the ignition lag decreases at high temperatures. They also reported that the increased pressure shortens the ignition lag for fuel-rich and stoichiometric mixtures. Another study conducted by Grigorean *et al.* [12], presented the simulation results of combustion of ethylene. They reported minimum CO emissions at 700K with an excess air ratio of 1.5, the pressure of 1 bar, while the maximum CO was observed at an 800K, I bar and excess air ratio of 1.5. Similarly, the maximum CO_2 was found to be at 700K, 3 bar, and excess air ratio of 3, while the lowest CO_2 was observed to be at 700K, 1 bar pressure, and 1.5 excess air ratio.

This study reports on the effect of utilising hydrogen fuel direct injection into a gasoline engine on performance, combustion, emissions and fundamental exergy and energy parameters. A four-cycle gasoline engine with a variable compression ratio of 9.5-10 was used for the numerical modelling. Special attention was given to the utilisation of a higher percentage of hydrogen fuels shared with iso-octane.

One of the key novelties of this study is to investigate why the exergy and energy parameters are higher for higher percentage hydrogen fuels than traditional gasoline (iso-octane) fuel. Secondly, a comprehensive examination was conducted of why hydrogen shared fuels with gasoline are sustainable in terms of depletion factor, sustainability index, and greenhouse gas (CO_2) emissions. The third vital novelties of this investigation are to find out the dominant factors for higher NOx emissions with hydrogen shared fuels. Finally, this investigation confirmed the principal causes of NOx formation by introducing another fuel, ethylene, into a gasoline engine. The main operating parameters investigated for NOx formation were excess air ratio, in-cylinder temperature, heat transfer rate, heat release rate and cumulative heat release.

To the best of the authors' knowledge, a comprehensive literature review revealed no articles were found that discussed the exergy, energy, exergy efficiency, sustainability index, depletion factor, unitary cost index, and CO_2 emissions for hydrogen fuels shared with iso-octane (neat gasoline). Additionally, no studies were found that discussed the associated factors for the causes of NOx formation.

II. METHODOLOGY

1-D modelling with GT-Suite and ANSYS was conducted for a four-stroke gasoline engine, where gasoline is injected directly while hydrogen is injected into the intake manifold for an engine speed of 1500 rpm. Furthermore, the modelling was carried out for excess air ratios of 1.1 to 1.5 with an increment of 0.1 for neat gasoline (reference fuel) and different hydrogen fuels. A snapshot of the methodology is shown in Figure 1.

A. MODELLING WITH GT-SUITE

As mentioned previously, some of the published experimental data were validated using GT-Suite and ANSYS software. The GT-Suite model was used to predict the in-cylinder pressure, heat release rate, cumulative heat release, and in-cylinder temperature. To check the accuracy of the model by GT-Suite, the in-cylinder pressure and temperature data were also compared with those obtained from ANSYS. The data variations between experiments and GT-Suite and ANSYS were within 5-10%. For any fuel, the following fuel property parameters shown in Table 1 are needed [13] to input into the software.

1-D modelling with GT-Suite involves the solution of the conservation of momentum, energy, and continuity equations. In the model, the engine system was discretised into volume numbers. The continuity, energy and momentum equations are shown in equations (i), (ii) and (iii), respectively [13]. For different notations, Greek symbols, and abbreviations

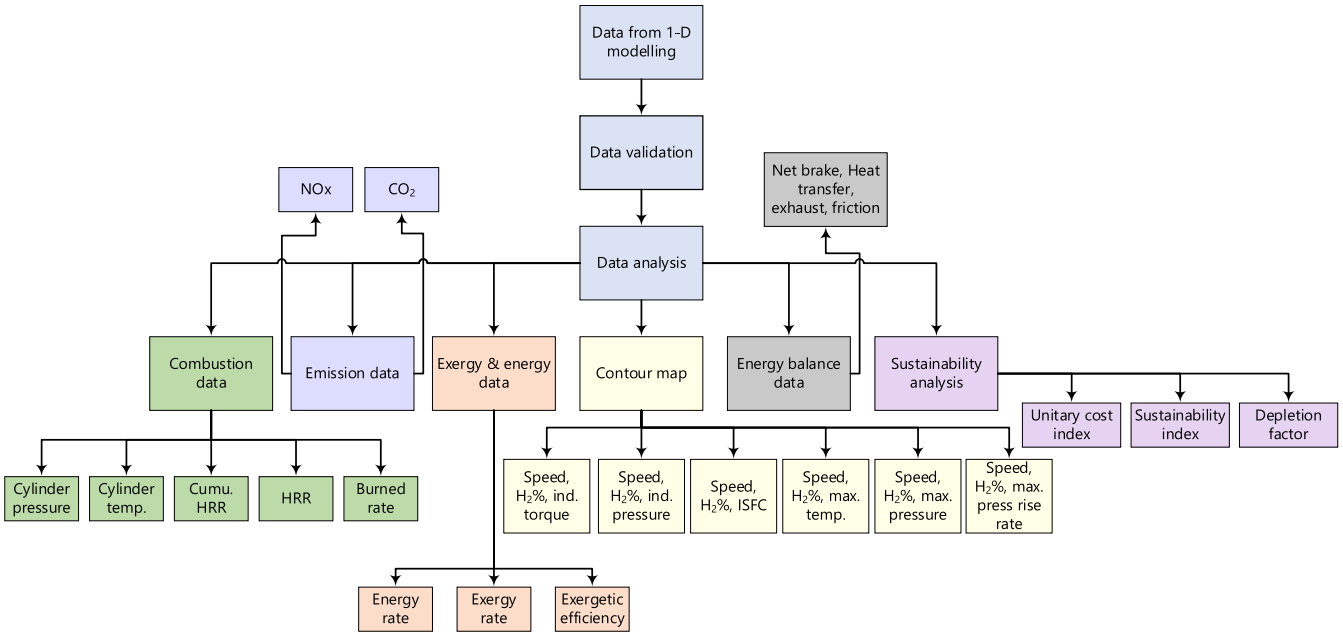

FIGURE 1. Methodology snapshot.

TABLE 1. Fuel's liquid and vapour property parameters.

State	Fuel property parameters
Liquid	Enthalpy Density, Dynamic viscosity Thermal conductivity Vapourisation heat
Vapour	Dynamic viscosity, Lower calorific value Critical pressure and temperature Thermal conductivity Enthalpy Oxygen, hydrogen, and carbon number

TABLE 2. Engine specifications for 1-D modelling.

Parameters	Value
Engine type	4-stroke gasoline
Bore (mm)	82.8
Stroke (mm)	84.0
Connecting rod (mm)	180
TDC clearance height (mm)	0.5
Compression ratio (-)	9.5-10
Gasoline	Port injection
Hydrogen	Direct injection

in equations (i-vi), the readers are referred to [13]. The specifications and schematic diagram for the 1-D modelling engine are shown in Table 2 and Figure 2, respectively (i)–(iii), as shown at the bottom of the page. The fuel flow rate was computed by equation (iv)

$$\dot{m}_{Delivery} = \eta_V \rho_{ref} N_{RPM} V_D \left(\frac{F}{A}\right) \frac{6}{(\#CYL)\,(Pulse\ width)} \tag{iv}$$

Woschini's equation for the convective heat transfer shown in equation (v), was used for the in-cylinder combustion model [13].

$$h_{c(Woschni)} = \frac{K_1 p^{0.8} w^{0.8}}{B^{0.2} T^{K_2}} \tag{v}$$

The burn rate was computed with Wiebe's function shown in equation (vi) [13].

$$Combustion = \left[1 - e^{(-WC)(\theta - SOC)^{(E+1)}}\right] \tag{vi}$$

where,

$\dot{m}$: boundary mass flux $= \rho A u$,

dp: pressure differential (across the length),

$$\frac{dm}{dt} = \sum_{boundaries} \dot{m} \tag{i}$$

$$\frac{D(me)}{dt} = -p\frac{dV}{dt} + \sum_{boundaries} (\dot{m}H) - hA_s(T_{fluid} - T_{Wall}) \tag{ii}$$

$$\frac{d\dot{m}}{dt} = \frac{dpA + \sum_{boundaries} (\dot{m}u) - 4C_f \frac{\rho u|u|}{2} \frac{dxA}{D} - K_p \left(\frac{1}{2}\rho u\,|u|\right) A}{dx} \tag{iii}$$

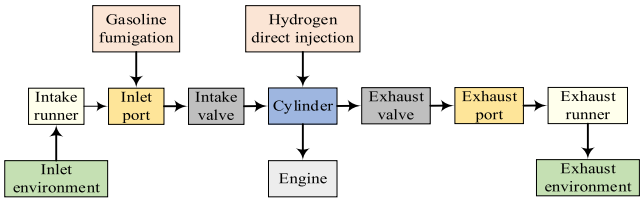

FIGURE 2. Schematic diagram for 1-D modelling engine.

dx: mass element length (in the flow direction),
H: specific enthalpy,
h: Coefficient of heat transfer,
A_s: heat transfer surface area,
A: flow area,
T_{fluid} and T_{wall} are the fluid and wall temperature,
u: boundary velocity,
m: mass of volume,
V: volume,
ρ : density,
K_p: pressure loss coefficient,
C_f: Fanning friction factor,
D: equivalent diameter,
$\dot{m}_{Delivery}$: Rate of delivery (injector),
N_{RPM}: Engine speed (rpm),
F/A: Fuel-air ratio,
#CYL: Cylinder number,
ρ_{ref}: reference density for volumetric efficiency,
η_v: volumetric efficiency,
Pulse width: duration of injection,
h_c: convective heat transfer coefficient,
K_1: constant,
B: bore of the cylinder,
T and p: cylinder temperature and pressure, respectively,
w: mean gas velocity,
θ : instantaneous crank angle,
CE: Fuel burned fraction,
WC: Constant (Wiebe),
SOC: Start of combustion,
E: Wiebe exponent.

B. MODELLING WITH ANSYS

A numerical simulation of an engine combustion model was developed with the help of ANSYS. For solving the turbulent model, Reynold's Average Navier-Stokes (RANS) method was used in this study. An Instantaneous Analog Analogy was adopted for disintegrating the variations and time-dependent average quantities. A rebound/Sliding model was created to resolve the interaction between the spray-wall. Another approach of using Re-Normalisation Group (RNG) K-epsilon was used to investigate the turbulence characteristics inside the cylinder. According to the previous study, more accurate and reliable results can be found using this approach [14]–[17]. Compressible turbulence can also be determined numerically by using this method which is established by the following equations.

$$\frac{d(\rho K)}{dt} = S - \rho_\varepsilon + D_k \quad \text{(vii)}$$

$$\frac{d(\rho \varepsilon)}{dt} = C_1 \frac{S\varepsilon}{K} - C_2 \rho \frac{\varepsilon^2}{K} + C_3 \rho (\varepsilon \times \cup) + D_\varepsilon \quad \text{(viii)}$$

Equations (vii) and (viii) are the dissipation rate equation ε and kinetic energy equation k. S denotes the turbulent energy generation, U represents the velocity vector, D_k and D_ε represent the turbulent diffusion, C is constant, and ρ is the fluid density (kg/m^3). The following parameters in Tables 3, 4, and 5 were considered for conducting the simulation [14], [17].

Figures 3(a-b) show the model geometry and mesh set-up.

TABLE 3. Solver set-up.

Parameters	Value
Model Type	3D turbulent model (k-epsilon)
Number of Cylinder	4
Bore	98 mm
Stroke Length	110 mm
Solver type	CFD
Simulation Type	Sector Combustion

TABLE 4. Meshing.

Parameters	Value
Mesh Type	Coarse
Element order	Quadratic
Maximum Element Size	1.7
Number of elements	91312
Number of Nodes	95810

TABLE 5. Boundary condition.

Parameters	Value
Variation of peak pressure against the benchmark	0.11% [14, 17]
Engine Speed	1500
Excess air ratio	1.5
Injection shape	trapezoidal wave
Injection Angle	70°
Wall temperature	313K (Constant) [14, 17]

III. RESULTS AND DISCUSSIONS

Figure 4 is a comparison of brake mean effective pressure (BMEP) between simulation results with the experiments conducted by Du *et al.* [9] for the neat gasoline (H_2_0%) and five hydrogen fractions for three excess air ratios (1.1, 1,2, 1.5). As seen in the Figure, the BMEP increases as hydrogen fraction increases for all three excess air ratios. As also seen from the Figure that higher excess air ratios show lower BMEPs, while the lowest excess air ratio, 1.1, offers the highest BMEP for both simulation and experimental data. The higher BMEP at a lower excess air ratio is due to a larger amount of fuel burned into the combustion chamber. BMEPs for both experimental and

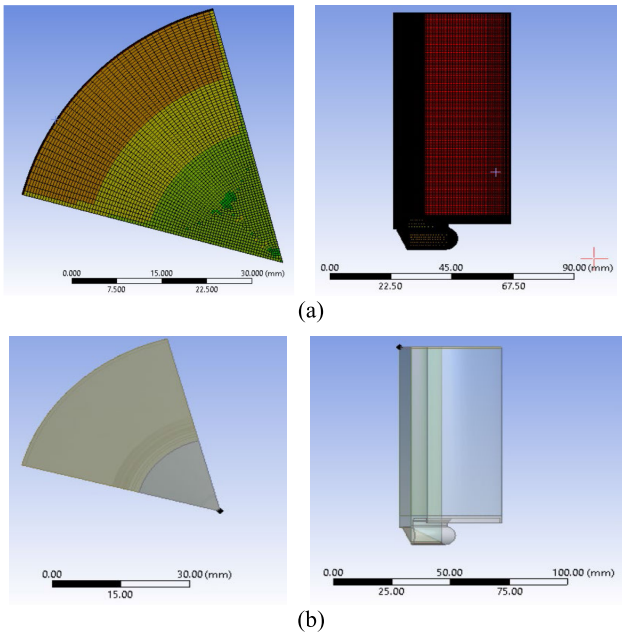

FIGURE 3. (a) Model geometry (b) Mesh set-up.

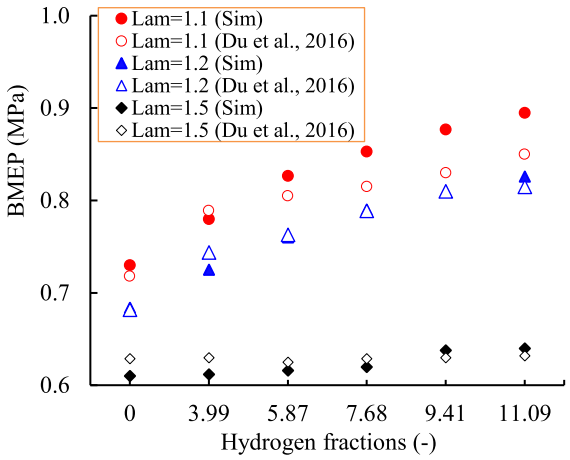

FIGURE 4. Comparison of predicted brake mean effective pressure (BMEP) with experimental BMEP results (adapted from Du *et al.* [9]).

simulation data are close enough for all excess air ratios and all hydrogen fractions. The highest variations of BMEP between experimental and simulated data are 5.88% for an excess air ratio of 1.1. The maximum variations between experimental and simulation results for excess air ratios of 1.2 and 1.5 are 1.88% and 3.02%. Based on the above discussion and comparison, it can be concluded that the predicted simulation results are in good agreement with those of the experimental results.

Figure 5 compares predicted (a) in-cylinder pressure and (b) in-cylinder temperature results using ANSYS and GT-Suite. The comparison was made for an excess air ratio of 1.5 and engine speed of 1500 rpm. It is widely accepted that excess air ratio is the ratio between the actual air to

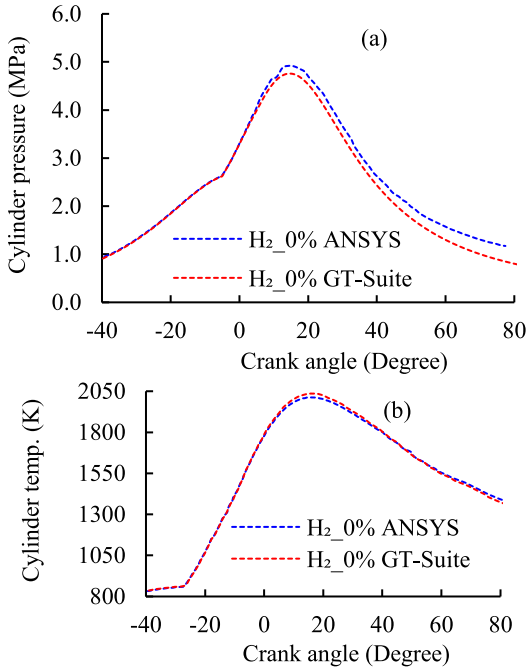

FIGURE 5. Comparison of (a) in-cylinder pressure and (b) in-cylinder temperature for ANSYS and GT-Suite for an excess air ratio of 1.5 and an engine speed of 1500 rpm.

fuel ratio and the stoichiometric air to fuel ratio. The reason for choosing excess air ratio (Lamda, shortened as Lam in Figure 4) is to compare the simulation results with published data, as the published data (discussed in Figure 4) of brake mean effective pressure (BMEP) versus hydrogen fractions were plotted for different excess air factors (1.1, 1.2, 1.5). The other reason for choosing excess air ratio is that the excess air ratio is an extensively used parameter to quantify whether the mixture of air and fuel in the combustion chamber is lean or rich. Both in-cylinder pressure and in-cylinder temperature results are almost identical for ANSYS and GT-Suite. The peak pressure was found to be 4.91 MPa for ANSYS and 4.75 MPa for GT-Suite. The percentage variations of peak cylinder pressure with ANSYS and GT-Suite are 3.35%. Figure 5(b) displays the in-cylinder temperature for the same excess air ratio of 1.5 using the same two software (ANSYS, GT-Suite). Insignificant variations in in-cylinder temperature are observed for the ANSYS and GT-Suite. The peak cylinder temperature with ANSYS is found to be 2035.47K, while for GT-Suite, the peak cylinder temperature was observed to be 2016.35K – the variations are less than 1%.

The exergy rates were estimated with the following equation:

$$\text{Exergy rate} = \phi \times \text{m}_\text{f} \times \text{fuels}' \text{ heating value} \qquad \text{(ix)}$$

where,

ϕ is the exergy factor; m_f is the mass flow rate of fuel.

The energy rate was computed using equation (x).

$$\text{Energy rate} = \text{m}_\text{f} \times \text{fuel}'\text{s heating value} \qquad \text{(x)}$$

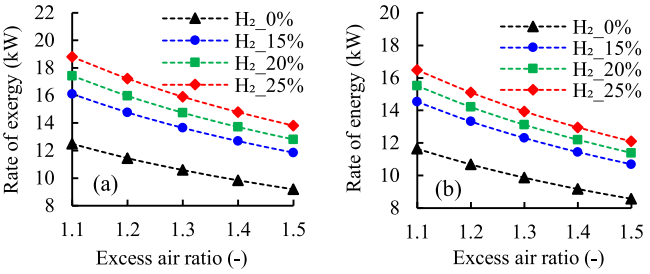

FIGURE 6. Influence of excess air ratio on the variations of (a) exergy rates; (b) energy rates for four fuels.

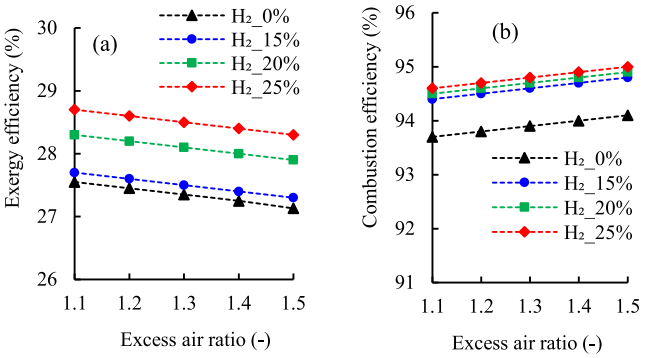

FIGURE 7. Influence of excess air ratio on the variations of (a) exergy efficiencies; (b) combustion efficiencies for four fuels.

Exergy efficiency calculation was based on equation (xi).

$$\text{Exergy efficiency} = \frac{\text{The energy flow accompanying work}}{\phi \times m_f \times \text{fuel's heating value}} \quad \text{(xi)}$$

The combustion efficiency was computed by using equation (xii).

$$\text{Combustion efficiency} = \frac{\overline{h_P} - \overline{h_R}}{|\text{Fuel's heating value}|} \quad \text{(xii)}$$

where $\overline{h_P}$ and $\overline{h_R}$ are enthalpies of product and reactant, respectively. The readers are referred to the references of Nabi, *et al.* [18] and Odibi *et al.* [19] for details to estimate exergy and energy parameters, including exergy rates, energy rates, thermal efficiency and combustion efficiency.

Figure 6(a) depicts the variations of exergy rates against excess air ratios for neat octane (H_2_0%) and three hydrogen fuels (H_2_15%, H_2_20%, H_2_25%). A general trend of decreasing exergy rate with the increase in excess air ratio is observed irrespective of the fuels or the percentage of hydrogen-shared with octane. An R-squared value (linear fit) of higher than 0.99 indicates a strong correlation between exergy rate and excess air ratio for all fuels. All hydrogen fuels show a higher exergy rate than that of neat gasoline (H_2_0%). As seen from the Figure, there is higher exergy on the leaner side (comparatively lower amount of air than the richer side). Relative to H_2_0%, a maximum of 28.98% increase in exergy rate is observed with an H_2_15% fuel at an excess air ratio of 1.1. For the same excess air ratio (1.1), the rise in exergy rate with the other two fuels (H_2_20% and H_2_25%) increases a maximum of 39.55% and 50.52%, respectively.

Similarly, for an excess air ratio of 1.5, the increment of the exergy rates with H_2_15%, H_2_20%, and H_2_25% are observed to be 28.1%, 39.1%, and 49.5%, respectively. The higher exergy rate with three hydrogen fuels is associated with the higher heating value of hydrogen than octane. Nabi *et al.* [20] reported higher exergy rates for fuels with higher heating values. The current investigation is aligned with the work of Nabi *et al.* [20].

The changes in energy rates to excess air ratios for neat octane (H_2_0%) and three hydrogen fuels (H_2_15%, H_2_20%, H_2_25%) are illustrated in Figure 6 (b). The decreasing trends of energy rates with the increase in excess air ratio are also noticed in Figure 6 (b) regardless of the types of fuels or the percentage of hydrogen-shared with octane. Like exergy rates, all three hydrogen fuels show a higher energy rate than neat octane (H_2_0%). Like exergy rate and excess air ratio, an R-squared value (linear fit) higher than 0.99 indicates a strong correlation between energy rate and excess air ratio for all fuels. The increases in energy rates at an excess air ratio of 1.1 using the three hydrogen fuels compared to H_2_0% are noted to be 24.1%, 33.2% and 41.6%, respectively. At an excess air ratio of 1.5, the associated increases are 23.8%, 32.9% and 40.9%. The present study is in good agreement with the investigation of [20]. The linear fit R-squared value indicates that both energy and exergy rates are dependent on excess air ratios.

The changes in exergy efficiency with excess air ratio are shown in Figure 7(a) for four fuels. For all fuels, as seen in the Figure, the exergy efficiencies are maximum at an excess air ratio of 1.1, where the fuel-rich region exists compared to other excess air ratios in the fuel-lean regions. The exergy efficiency for fuel with 0% hydrogen share shows the lowest excess air ratios, while the 25% shared hydrogen fuel exhibit the highest exergy efficiency at all excess air ratios. The two other hydrogen fuels also show higher exergy efficiencies than baseline gasoline (H_2_0%) for the same operating conditions. At an excess air ratio of 1.5, H_2_0% fuel shows an exergy efficiency of 27.13%, while the three hydrogen fuels (H_2_15%, H_2_20% and H_2_25%) show 27.3%, 27.9% and 28.3%, respectively. Relative to H_2_0% fuel, at an excess air ratio of 1.5, the three hydrogen fuels increase in exergy efficiencies by 0.65%, 2.9% and 4.30%, respectively. The lowest increases in exergy efficiencies at an excess air ratio of 1.1 with H_2_15%, H_2_20%, and H_2_25% fuels are 0.54%, 2.7% and 4.1%, respectively. The results of Figure 7(a) indicate the advantage and suitability of using a higher percentage of hydrogen fuel concerning exergy efficiency. Relative to H_2_0% fuel, a 4.3% increase in exergy efficiency with H_2_25% fuel is significantly high.

Figure 7(b) illustrates combustion efficiencies to excess air ratios for the same four fuels as shown in the previous

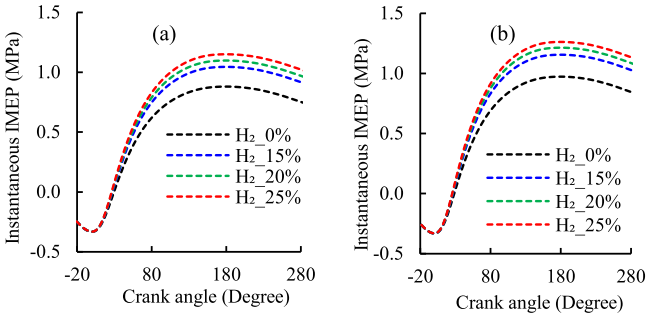

FIGURE 8. Instantaneous IMEP for excess air ratios of (a) 1.5, and (b) 1.3 for three hydrogen and neat gasoline fuels.

Figures. It is well-known that higher combustion efficiencies of a fuel indicate better combustion, leading to a lower level of combustion products. Figure 7(b) shows higher combustion efficiencies at higher excess air ratios for all fuels investigated in this study. H_2_0% shows combustion efficiencies of 93.7%, 93.81%, 93.93%, 94% and 94.1% at excess air ratios of 1.1, 1.2, 1.3, 1.4, and 1.5, respectively. H_2_15% indicates slightly higher combustion efficiencies than H_2_0% fuel at the same five excess air ratios. H_2_20% reveals better than H_2_15% and H_2_0% fuels. Fuel H_2_25% shows the highest combustion efficiencies among four fuels at all excess air ratios.

Figures 8(a) and 8(b) are the support data of instantaneous indicated mean effective pressure (IMEP), indicating why hydrogen fuel blends have higher thermal efficiencies compared to neat gasoline fuel. Figure 8(a) shows the instantaneous IMEP for an excess air ratio of 1.5, while Figure 8(b) for an excess air ratio of 1.3 for neat gasoline and three higher-fraction hydrogen blends. It is generally accepted that the indicated mean effective pressure is generated into the cylinder, and it is an indication of the capability of doing work. As can be seen from the Figure, the instantaneous IMEP for neat gasoline is the lowest for all four fuels, while the higher-fraction hydrogen fuels (H_2_25%) show the highest. For an excess air ratio of 1.5, neat gasoline shows a maximum IMEP of 0.88 MPa at a crank angle of 188 degrees. The three higher-fraction hydrogen blends (H_2_15%, H_2_20% and H_2_25%) show the IMEP values of 1.045 MPa, 1.098 MPa and 1.15 MPa at crank angles of 188°, 180.05°, 179.68° and 179.48°, respectively. Interesting to note that the peak of the IMEP for hydrogen blends shifts from right to left. The shifting is prominent for the higher-fraction hydrogen blend–H_2_25% in this case. This indicates the faster combustion with hydrogen fuel blends compared to neat gasoline fuels. Similar trends are observed for the same four fuel blends at an excess ratio of 1.3. At an excess air ratio of 1.3, the IMEP for neat gasoline is observed to be 0.973 MPa at a crank angle of 180.64°. The same three hydrogen blends show the IMEP values of 1.155 MPa, 1.213 MPa and 1.26 MPa at crank angles of 180.64°, 179.51°, 179.45° and 179.30°, respectively. Also, it can be noted that a lower excess air ratio (1.3) shows higher IMEP for all fuels compared to a higher excess air ratio of

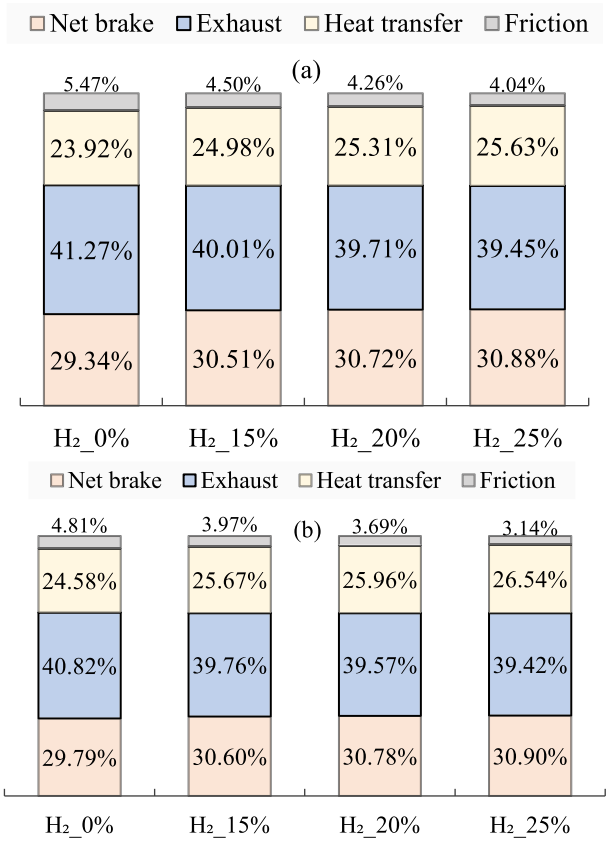

FIGURE 9. Energy balance for the four fuels for excess air ratios of (a) 1.5 and (b) 1.3 for three hydrogen and gasoline fuels.

1.5. Compared to neat gasoline, at an excess air ratio of 1.5, a maximum of 19% increase in IMEP was observed with H_2_15% fuel. The H_2_20% and H_2_25% increase IMEPs by 25% and 31%. Almost similar percentages (18.5%, 24.98% and 30%) increase in IMEPs were realised for an excess air ratio of 1.3 for the same three hydrogen blends relative to neat gasoline fuel. Based on the discussion in Figure 8, it can be concluded that higher-fraction hydrogen fuels realised much higher IMEPs which in turn suggest the higher thermal efficiency.

The energy balance for three hydrogen fuels and gasoline is displayed in Figure 9. The results are plotted for excess air ratios of 1.5 and 1.3. The energy balance results for the other excess air ratios (not shown) also reveal similar trends.

As seen in Figure 9, the net brake and heat transfer for all three hydrogen fuels are higher compared to gasoline at both excess air ratios, while the friction and exhaust losses are lower at both excess air ratios. The higher net brake and heat transfer and lower friction and exhaust losses with the three hydrogen fuels are the additional causes of higher thermal efficiencies than gasoline.

Figure 10 is a contour map interpretation for the three hydrogen fuels and reference gasoline as indicated. For mapping these contours, the excess air ratio was kept constant at 1.1. More specifically, the engine speed varied from 1400 rpm to 2400 rpm. The hydrogen fractions were kept at

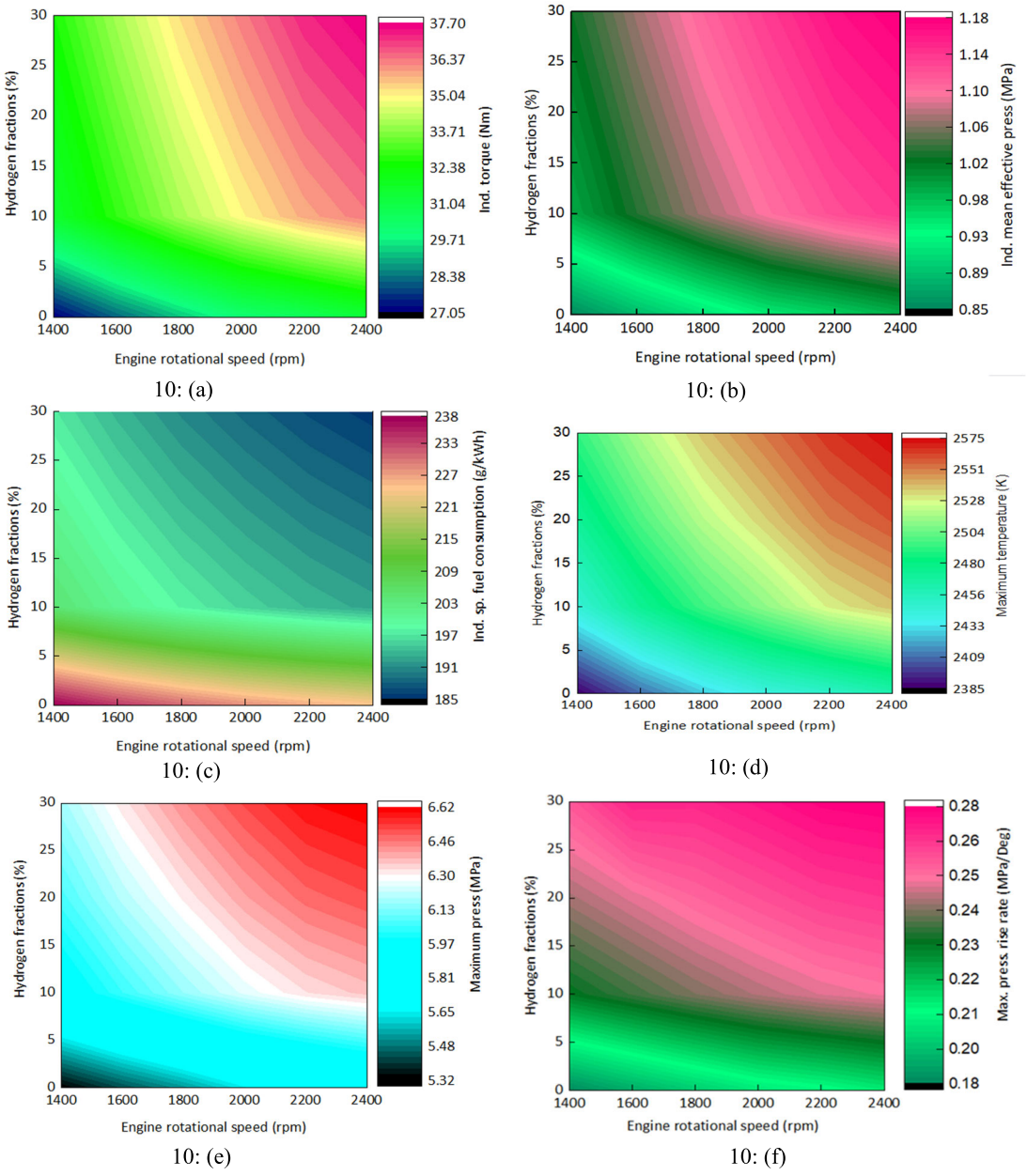

FIGURE 10. **Contour map for hydrogen fraction, engine rotational speed and (a) indicated torque; (b) indicated mean effective pressure (IMEP); (c) indicated specific fuel consumption (ISFC); and (d) maximum in-cylinder temperature; (e) maximum pressure; (f) maximum pressure rise rate.**

0%, 15%, 20% and 30%, while the excess air ratio was fixed at 1.1. The contours for other excess air ratios show (results not shown) similar trends. As seen in Figure 10(a), the lowest indicated torque was observed at a hydrogen fraction of 0% with an engine rotational speed of 1400 rpm.

Higher than 0% hydrogen fraction, the indicated torque increases significantly at all engine speeds. It is also noticed that the higher than 0% hydrogen fraction and at higher engine rotational speed, the indicated torque becomes higher. From the Figure, the highest indicated torque is observed to be at an engine speed of 2400 rpm with a hydrogen fraction of 30%. Also, as per the contour map, the H_2_10% could be the optimum hydrogen fraction in terms of indicated torque. From Figure 10(b), similar results can be observed for the same three hydrogen fuels, and reference gasoline for indicated mean effective pressure (IMEP). Figure 10(c) maps the predicted specific fuel consumption (ISFC) for engine rotational speed and hydrogen fractions. Interestingly, at the lower engine speed with a zero percent hydrogen fraction (H_2_0%, reference gasoline), the ISFC is maximum. The opposite can be found for H_2_30% fuel from the same plot. 30% hydrogen fraction (H_2_30%) at an engine speed

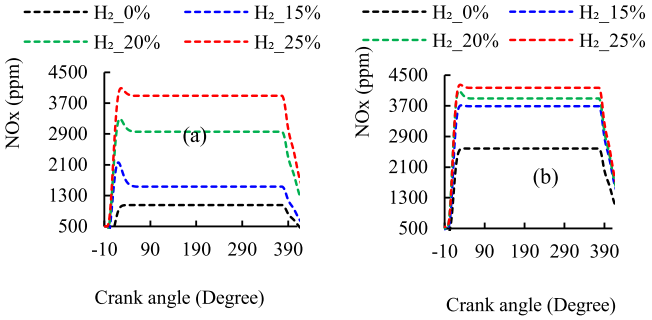

FIGURE 11. Variations of NOx emissions for excess air ratios of (a) 1.5 and (b) 1.3 for neat gasoline and three hydrogen fuels.

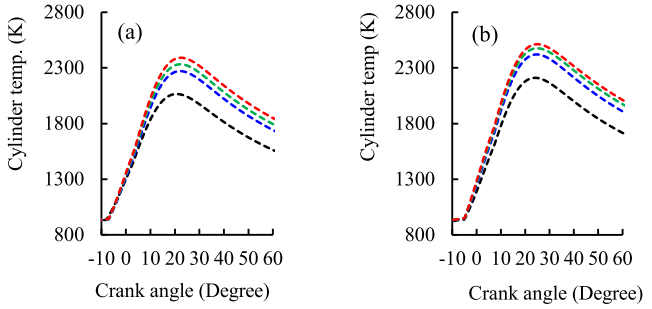

FIGURE 12. Variations of NOx emissions for excess air ratios of (a) 1.5 and (b) 1.3 for neat gasoline and three hydrogen fuels. For figure legends, please refer to Figure 7.

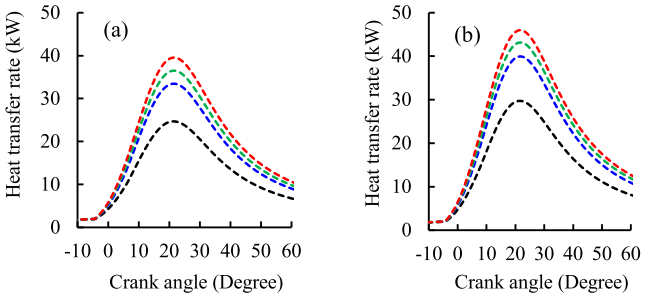

FIGURE 13. Variations of heat transfer rate for excess air ratios of (a) 1.5 and (b) 1.3 for neat gasoline and three hydrogen fuels. For Figure legends, please refer to Figure 7.

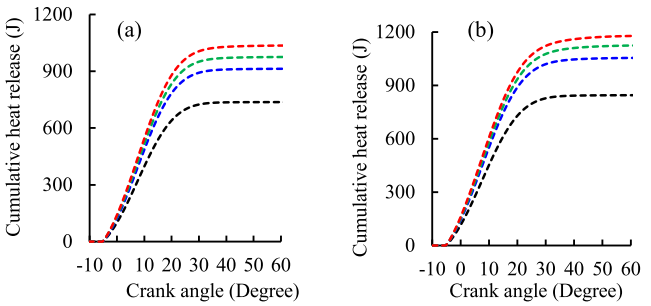

FIGURE 14. Variations of cumulative heat release for excess air ratios of (a) 1.5 and (b) 1.3 for neat gasoline and three hydrogen fuels. For figure legends, please refer to Figure 7.

of 2400 rpm indicates the lowest ISFC. An intermediate value of ISFC is observed for hydrogen fractions of 0% - 30%. Maximum in-cylinder temperature mapping for engine rotational speed and hydrogen fractions is illustrated in Figure 10(d). Like IMEP and ISFC, the in-cylinder heat transfer map realises (results not shown) the highest at 2400 rpm with 30% hydrogen fraction and the lowest at 0% hydrogen fraction at an engine rotational speed of 1400 rpm. Maximum in-cylinder pressure is plotted against hydrogen fractions and engine rotational speed (Figure 10(e)) for an excess air ratio of 1.1 like Figures 10(a)-10(d), maximum pressure in Fig 10(e) shows the lowest for H_2_0%, while the maximum for H_2_25%. The higher maximum pressure with hydrogen fuels leads to higher thermal efficiency. Figure 10(f) is the contour plot of the maximum pressure rise rate with respect to hydrogen fractions and engine rotational speed. It is clear from the Figure that the higher the hydrogen fractions, the higher the maximum pressure rise rate. Also, the maximum pressure rise rate is higher at higher engine speeds for all fuels.

The plots in Figure 11 present the changes in NOx emissions for excess ratios of 1.5 (Fig. 11a) and 1.3 (Fig. 11b) for the three hydrogen fuels (with hydrogen) and gasoline (without hydrogen). It is generally accepted that the formation of NOx mainly depends on high flame temperature, oxygen content, injection parameters and properties of fuel [21]. As evident from the Figure, the NOx emissions for hydrogen fuels are higher compared to gasoline. A notable increase in NOx emissions is observed for both excess ratios with three hydrogen fuels. The increase is significant for a higher percentage of hydrogen fractions. The increase in NOx emissions with H_2_15% is 1.40 fold higher compared to gasoline at an excess air ratio of 1.5. H_2_20% and H_2_25% fuels increase NOx emissions by 2.8 and 3.6 fold at an excess ratio of 1.5. The corresponding figures for the three hydrogen fuels for an excess air ratio of 1.3 are 1.42, 1.50 and 1.60 fold, respectively. The increase in NOx emissions with hydrogen fuels is due to higher in-cylinder temperature, higher heat transfer rate, and higher cumulative heat release relative to reference gasoline fuel. The higher in-cylinder temperature with hydrogen fuels for the two excess air ratios (1.3 and 1.5) are displayed in Figure 12. As anticipated, the higher in-cylinder temperature is realised at an excess air ratio of 1.3 compared to 1.5 for all fuels investigated in this study. This is associated with a higher amount of fuel being burned at a lower excess air ratio, 1.3, in this case. According to the Zeldovich NOx formation phenomenon, the higher in-cylinder temperature is associated with higher NOx formation using three hydrogen fuels. The other factors for higher NOx emissions are heat transfer rate and cumulative heat release, as seen in Figures 13 and 14. The heat transfer rate in Figure 13 for an excess air ratio of 1.5 with the three hydrogen fuels is observed to be increased by 1.35, 1.47, and 1.60 times, while for the excess air ratio of 1.3, the corresponding values are 1.33, 1.45, and 1.54, respectively. Similarly, the cumulative heat release in Figure 14 for the same three hydrogen fuels is noted to be 1.23, 1.32, and 1.40 times higher than gasoline at an excess air ratio of 1.5.

Almost similar values (1.24, 1.33, and 1.39 times higher cumulative heat release) are observed at an excess air ratio of 1.3 for the H_2_15%, H_2_20% and H_2_25% hydrogen fuels, respectively. In reality, regardless of fuels or fuel types, the key contributions to NOx generation are the temperature of the gas flame, the time of fuel injection, residence time, and the characteristics of the fuel [22]. The current study reveals the same about NOx formation and supports this phenomenon. The NOx emissions with hydrogen shared fuels are higher due to higher in-cylinder temperature and other associated factors described above compared to those without hydrogen fuel.

A. SUSTAINABILITY OF HYDROGEN SHARED FUELS

The depletion factor and sustainability index are related to each other and are estimated by the equations (xiii) and (xiv), respectively [23], whereas the unitary cost index was computed by equation (xv) [18].

$$\text{Depletion factor (number)} = 1 - \text{exergy efficiency} \quad \text{(xiii)}$$

$$\text{Sustainability index} = 1/\text{depletion factor (number)} \quad \text{(xiv)}$$

$$\text{Unitary cost index} = 1/\text{exergy efficiency} \quad \text{(xv)}$$

As seen in Figure 15(a), the sustainability index decreases with the excess air ratio for all fuels. While showing the highest sustainability index at the lowest excess air ratio, the minimum sustainability index is observed at the highest excess air ratio for the same fuels. Compared to neat gasoline (H_2_0%), all hydrogen fuels show a higher sustainability index at all excess air ratios. Also, compared to hydrogen fuels, a higher sustainability index is observed with the higher hydrogen percentage in the blends. The higher sustainability index with all hydrogen fuels indicates that they are sustainable fuels for the internal combustion engine – gasoline engine in this investigation. Figure 15(b) displays the depletion factor, which was estimated with equation (xiii), for neat gasoline and three hydrogen fuels at excess air ratios of 1.1, 1.2, 1.3, 1.4, and 1.5. A close look at equation (xiv), the depletion factor has a reciprocal relation to the sustainability index. This suggests that the higher the depletion number, the lower the sustainability index of a particular fuel. The gasoline fuel (iso-octane, H_2_0%) shows the highest depletion factor at all excess air ratios, while H_2_25% fuel shows the lowest. The higher depletion factor with gasoline fuel results in being environmentally unsustainable. Figure 15(c) displays the unitary cost index of the four fuels for five different excess air ratios. The unitary cost index implies the minimum amount of exergy required by an internal combustion engine to produce one exergy unit of product [18]. The unitary cost index for all fuels was estimated by using equation (xv). Compared to neat gasoline, all three hydrogen fuels show a lower unitary cost index at all excess air ratios. At an excess air ratio of 1.5, the unitary cost index for the three hydrogen fuels is 3.66, 3.58, 3.53, while for neat gasoline is 3.69. The lower-cost index with

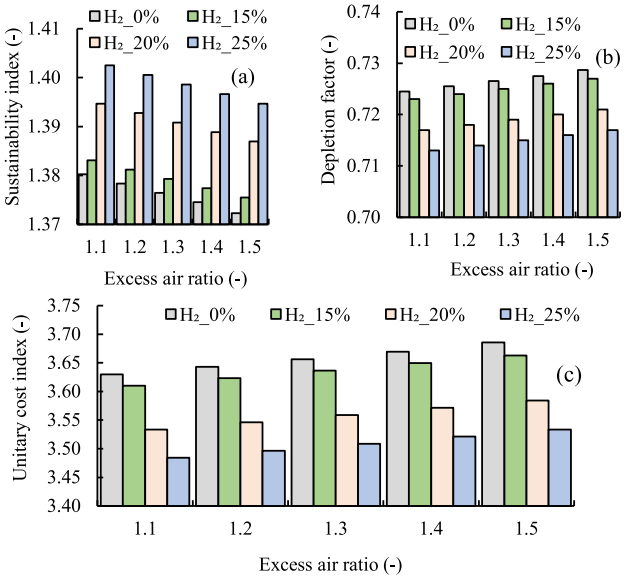

FIGURE 15. (a) Sustainability index; (b) depletion factor, and (c) unitary cost index for four fuels.

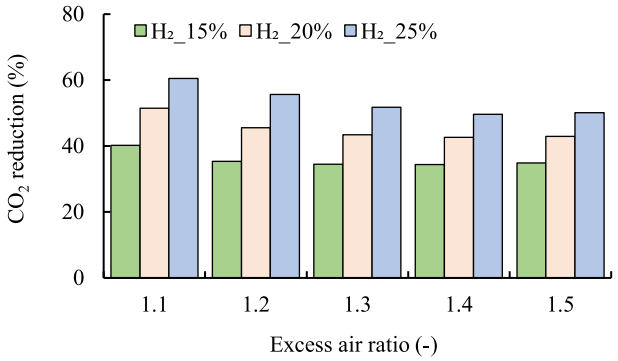

FIGURE 16. Changes in greenhouse gas (CO_2) emissions for neat gasoline and three hydrogen fuels for five excess air ratios.

hydrogen fuels compared to gasoline confirms the suitability of using hydrogen fuels as internal combustion engine fuels again.

The variations in greenhouse gas (CO_2) emissions at different excess air ratios for the four fuels are illustrated in Figure 16. Compared to neat gasoline, all three hydrogen fuels reduced CO_2 emissions significantly. Interestingly, the higher hydrogen fraction fuel (H_2_25%) reduced the highest CO_2 emissions at all five excess air ratios. At an excess air ratio of 1.1, H_2_25% reduced CO_2 emissions by 60.48% compared to H_2_0%. H_2_20% and H_2_15% reduced CO_2 emissions by 51.44% and 40.24%, respectively. Similarly, at an excess air ratio of 1.5, the reductions of CO_2 emissions by three hydrogen fuels (H_2_25%, H_2_20%, H_2_15%) are 49.5%, 42.95%, and 34.86%, respectively. A 60.48% greenhouse gas emission (CO_2) reduction with H_2_25% is an impressive achievement from this research.

Figure 17(a) is a depiction of CO_2 emissions and sustainability index (SI) against exergy efficiency. This Figure is a representation of an interesting finding of this

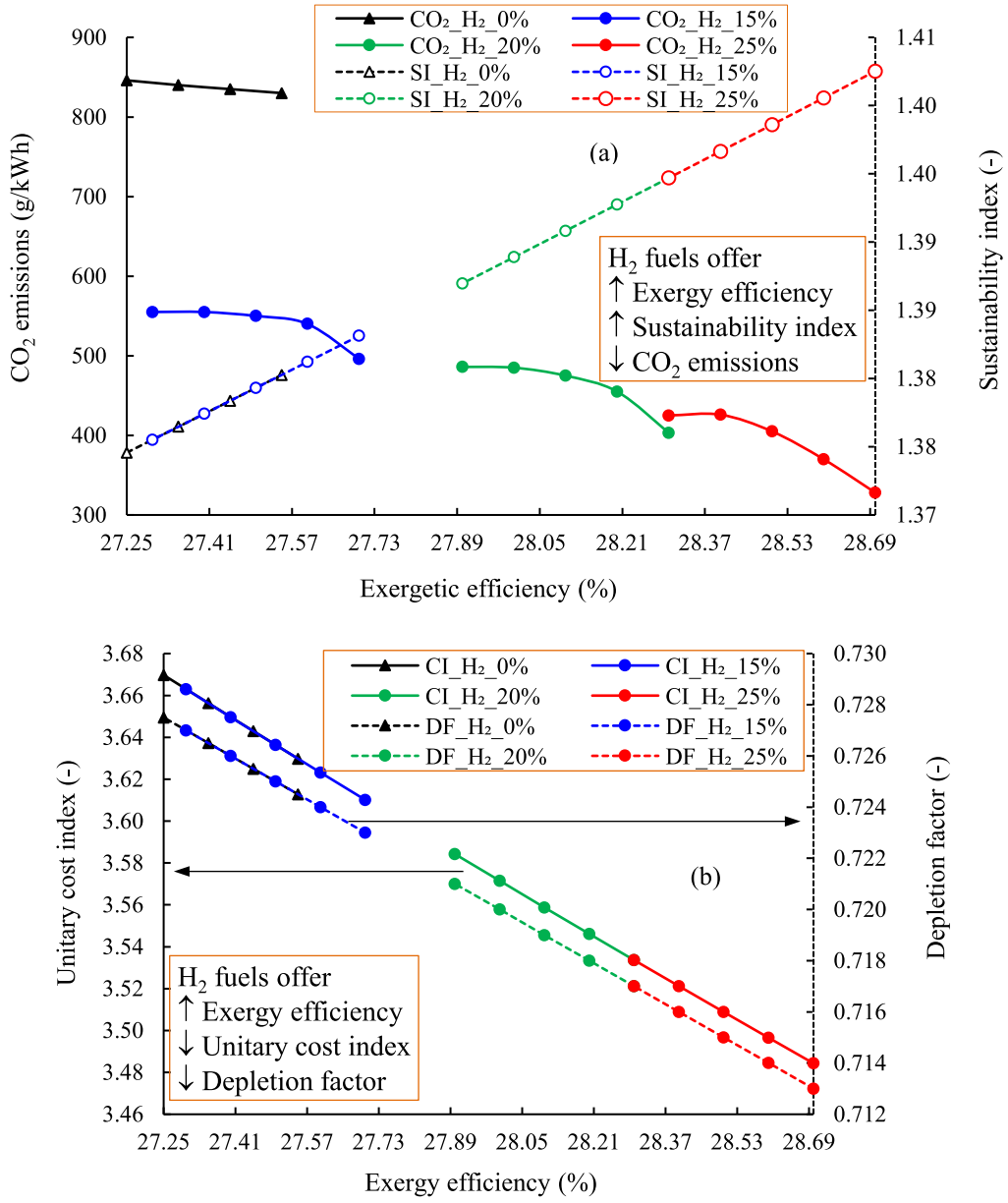

FIGURE 17. (a) Relationship between CO_2 emissions, sustainability index (SI) and exergy efficiency, (b) Relationship between unitary cost index (CI), depletion factor (DF) and exergy efficiency for neat gasoline and three hydrogen fuels for five excess air ratios.

study. As seen in the Figure, all hydrogen fuels exhibit higher exergy efficiencies and sustainability indices and substantially lower CO_2 emissions than neat gasoline fuel. Higher exergy efficiency improved sustainability index, and reduced impact on the environment (lower CO_2 emissions) with hydrogen fuels are some of the novel findings of this study. The current investigation is in good agreement with BoroumandJazi *et al.* [24].

The plots of unitary cost index and depletion factor/potential (DF) versus exergy efficiency are illustrated in Figure 17(b). The unitary cost index, also known as the unitary exergy cost index (CI), is the amount of exergy required by an engine (in this case, an internal combustion engine) to generate one exergy unit of product [18]. The depletion factor and the unitary exergy cost index were estimated using equations (xiii) and (xv), respectively. As can be seen in Figure 17(b), both unitary cost indices and depletion factors decrease with the increase in exergy efficiencies. Also, the magnitude of reductions in exergy cost index and depletion factor is higher for the higher-fraction hydrogen fuels than neat gasoline. A close look at equation (xv) discloses that the cost index has a reciprocal relationship with exergy efficiency. This indicates that the higher the exergy efficiency, the lower the exergy cost index

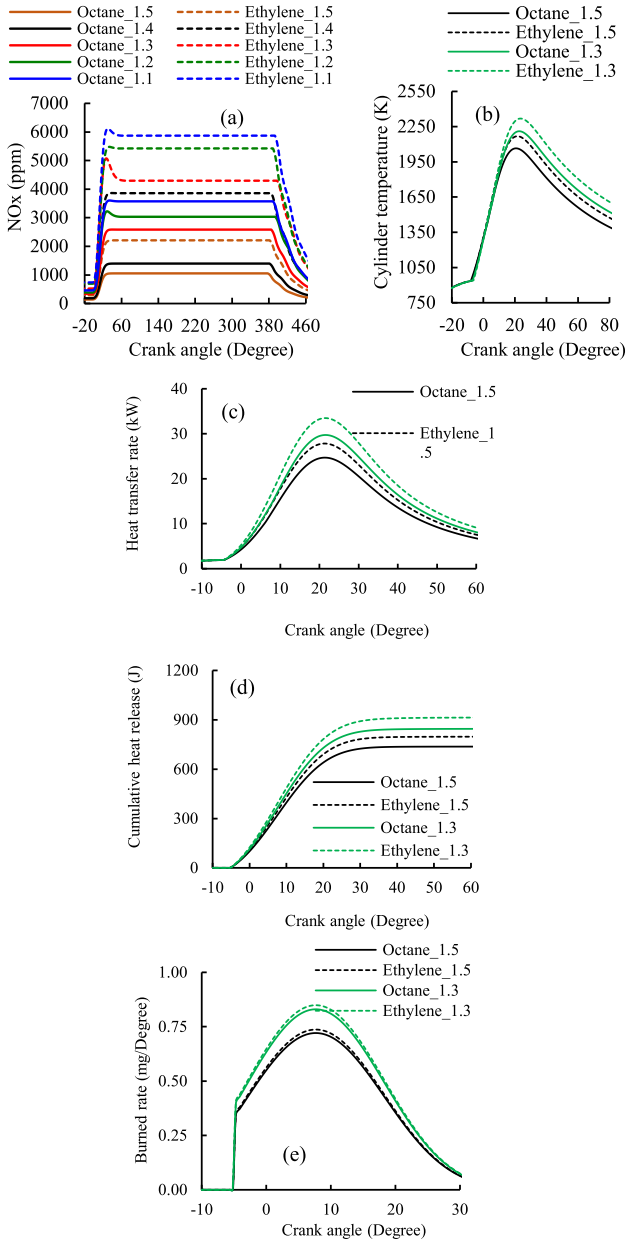

FIGURE 18. Comparison of (a) NOx emissions using neat gasoline and neat ethylene for five excess air ratios; and comparison of (b) cylinder temperature, (c) heat transfer rate, (d) cumulative heat release, and (e) burned rate with neat gasoline and neat ethylene for two excess air ratios (1.5 and 1.3).

is. As hydrogen fuels exhibit higher exergy efficiencies, they show lower exergy cost indices compared to neat gasoline fuel. The reason for lower depletion factors with hydrogen fuels is due to their higher exergy efficiencies.

In regards to sustainability analysis and discussion in Figures 17(a-b), all hydrogen fuels show higher sustainability indices, significantly lower greenhouse gas (CO_2) emissions, higher exergy efficiencies, lower depletion potentials (factors), lower exergy cost indices, which are some of the key contributions of this study that could help the vehicle manufactures and fuel researchers.

B. INVESTIGATION FOR NOx FORMATION

In this section, the NOx formation mechanism and its associated factors are confirmed again with gasoline (iso-octane, H_2_0%) and neat ethylene (C_2H_4).

It is well-known that NOx formation mechanisms are three types, including thermal NOx, prompt NOx and fuel NOx [25]. Among the three types of NOx formation, the thermal NOx is dominant for NOx formation inside the combustion chamber. In this phenomenon, the air nitrogen and oxygen combine and form NOx at high temperatures in the combustion chamber. The thermal NOx forms in the combustion chamber as per the Zeldovich mechanism as follows [25]:

$$O+N_2 \xleftrightarrow{k_1} N+NO;$$
$$N+O_2 \xleftrightarrow{k_2} O+NO;$$
$$N+OH \xleftrightarrow{k_3} H+NO.$$

In the above three equations, k_1, k_2, and k_3 represent the forward reaction rate constants.

The variations in NOx emissions with ethylene fuel and gasoline are depicted in Figure 18(a). NOx emissions for ethylene fuel are higher at all excess air ratios compared to gasoline. Also, it is evident from the Figure that at a lower excess air ratio, the NOx formation is also higher. This trend is valid for both fuels. As per the Zeldovich NOx formation mechanism [25], the higher NOx emissions with ethylene fuel are due to the higher in-cylinder temperature (Figure 18b) than gasoline. The current investigation agrees with the investigation conducted by Nabi *et al.* [14]. The other factors for higher NOx emissions with ethylene are the higher heat transfer rate, cumulative heat release and burned rate (Figures 18c, 18d, 18e). As explained before, like in-cylinder pressure and NOx formation, the in-cylinder temperature, heat transfer rate, cumulative heat release and burned rate for all fuels are higher at an excess air ratio of 1.3 than an excess air ratio of 1.5. This is due to fuel-rich conditions at lower excess ratios than fuel-lean conditions at higher excess air ratios. Again, these results indicate the different factors (in-cylinder temperature, heat transfer rate, cumulative heat release) that cause NOx formation.

IV. CONCLUSION

One-dimensional modelling for engine performance, NOx and CO_2 emissions for reference gasoline and three hydrogen fuels was conducted using GT-Suite and ANSYS software. The simulation results with GT-Suite were validated with those of ANSYS and published experimental results. The share of higher-fraction hydrogen fuels gives some novel findings. The addition of the fundamental exergy, energy parameters and sustainability analysis, including sustainability index, depletion number, unitary cost index, were additional novelties of this study. In the second part of this study, in-cylinder pressure, NOx emission, and its associated factors of formation were further investigated with neat

ethylene and reference gasoline. The results are summarised as follows:

- The lower-fraction hydrogen fuels (H_2_3.99%, H_2_5.87%, H_2_7.68%, H_2_9.41%, and H_2_11.09%) have a good agreement in BMEPs between simulation and experimental results. In-cylinder pressure and temperature data also have a good alignment between GT-Suite and ANSYS.
- The exergy efficiency, rate of exergy and energy, and combustion efficiencies for the three hydrogen fuels (H_2_15%, H_2_20% and H_2_25%) are significantly higher than those of the reference gasoline (H_2_0%).
- The instantaneous indicated mean effective pressure was found to be substantially higher compared to neat gasoline, which resulted in higher thermal efficiencies with higher-fraction hydrogen fuels.
- The CO_2 emissions with the same three hydrogen fuels are considerably lower, but the NOx emissions are notably higher than the reference gasoline for the same three hydrogen fuels. A maximum of 51% reduction in CO_2 emissions was observed with hydrogen fuel. The higher NOx emissions were associated with the higher in-cylinder temperature, higher heat transfer rate, higher cumulative heat release. On the other hand, the lower CO_2 emissions with the hydrogen fuels were due to lower carbon content in the hydrogen fuels.
- The sustainability indices are higher, depletion factor and the unitary cost indices are lower for all hydrogen-shared fuels than gasoline. Besides lower CO_2 emissions, these sustainability indices further proved that hydrogen fuels are both economically and environmentally sustainable.
- To confirm the NOx formation factors, the endeavour further evident that the higher NOx emissions with neat ethylene fuel were associated with the higher in-cylinder temperature, higher heat transfer rate, higher cumulative heat release and higher burned rate.

REFERENCES

[1] M. Rebai, S. Kelouwani, Y. Dube, and K. Agbossou, "Low-emission maximum-efficiency tracking of an intelligent bi-fuel hydrogen–gasoline generator for HEV applications," *IEEE Trans. Veh. Technol.*, vol. 67, no. 10, pp. 9303–9311, Oct. 2018.

[2] S. Simsek, S. Uslu, and H. Simsek, "Evaluation of the effect of a new alternative fuel containing boron and hydrogen on gasoline engine performance and emission responses," *Int. J. Environ. Sci. Technol.*, vol. 19, no. 6, pp. 4913–4922, Jun. 2022.

[3] Z. Qin, Z. Yang, C. Jia, J. Duan, and L. Wang, "Experimental study on combustion characteristics of diesel-hydrogen dual-fuel engine," *J. Thermal Anal. Calorimetry*, vol. 142, no. 4, pp. 1483–1491, 2020.

[4] S. Pukalskas, D. Kriaučiūnas, A. Rimkus, G. Przybyła, P. Droździel, and D. Barta, "Effect of hydrogen addition on the energetic and ecologic parameters of an Si engine fueled by biogas," *Appl. Sci.*, vol. 11, no. 2, p. 742, Jan. 2021.

[5] R. S. Kumar, M. Loganathan, and E. J. Gunasekaran, "Performance, emission and combustion characteristics of CI engine fuelled with diesel and hydrogen," *Frontiers Energy*, vol. 9, no. 4, pp. 486–494, Dec. 2015.

[6] S. Nag, P. Sharma, A. Gupta, and A. Dhar, "Combustion, vibration and noise analysis of hydrogen-diesel dual fuelled engine," *Fuel*, vol. 241, pp. 488–494, Apr. 2019.

[7] A. Cernat, C. Pana, N. Negurescu, G. Lazaroiu, C. Nutu, and D. Fuiorescu, "Hydrogen—An alternative fuel for automotive diesel engines used in transportation," *Sustainability*, vol. 12, no. 22, p. 9321, Nov. 2020.

[8] Y. Karagöz, T. Sandalcı, L. Yüksek, A. S. Dalkılıç, and S. Wongwises, "Effect of hydrogen–diesel dual-fuel usage on performance, emissions and diesel combustion in diesel engines," *Adv. Mech. Eng.*, vol. 8, no. 8, Aug. 2016, Art. no. 168781401666445.

[9] Y. Du, X. Yu, J. Wang, H. Wu, W. Dong, and J. Gu, "Research on combustion and emission characteristics of a lean burn gasoline engine with hydrogen direct-injection," *Int. J. Hydrogen Energy*, vol. 41, no. 4, pp. 3240–3248, Jan. 2016.

[10] J.-C. Martin, P. Millington, B. Campbell, L. Barron, and S. Fisher, "On-board generation of hydrogen to improve in-cylinder combustion and after-treatment efficiency and emissions performance of a hybrid hydrogen–gasoline engine," *Int. J. Hydrogen Energy*, vol. 44, no. 25, pp. 12880–12889, May 2019.

[11] Z. Wan, Z. Zheng, Y. Wang, D. Zhang, P. Li, and C. Zhang, "A shock tube study of ethylene/air ignition characteristics over a wide temperature range," *Combustion Sci. Technol.*, vol. 192, no. 12, pp. 2297–2305, Dec. 2020.

[12] S. Grigorean, G. Dumitrascu, and S. Predoi, "Oxy-combustion simulation of ethylene," in *Proc. IOP Conf., Mater. Sci. Eng.*, vol. 595, 2019, Art. no. 012014.

[13] M. N. Nabi, M. Rasul, and P. Gudimetla, "Modelling and simulation of performance and combustion characteristics of diesel engine," *Energy Proc.*, vol. 160, pp. 662–669, Feb. 2019.

[14] M. N. Nabi, M. G. Rasul, M. A. Arefin, M. W. Akram, M. T. Islam, and M. W. Chowdhury, "Investigation of major factors that cause diesel NO_x formation and assessment of energy and exergy parameters using e-diesel blends," *Fuel*, vol. 292, May 2021, Art. no. 120298.

[15] W. K. Hussam, M. N. Nabi, M. W. Chowdhury, M. E. Hoque, A. B. Rashid, and M. T. Islam, "Fuel property improvement and exhaust emission reduction, including noise emissions, using an oxygenated additive to waste plastic oil in a diesel engine," *Biofuels, Bioproducts Biorefining*, vol. 15, no. 6, pp. 1650–1674, Nov. 2021.

[16] C. Xu;, H. Cho;, and D. H. Park, "Effect of different fuels on combustion and emission components of CI engines," *Int. J. Mech. Prod. Eng. Res. Development.*, vol. 9, no. 6, pp. 821–834, 2019.

[17] M. T. Islam, F. Rashid, and M. A. Arefin, "Numerical analysis of the performance and NO_x emission of a diesel engine fueled with algae biofuel-diesel blends," *Energy Sour. A, Recovery, Utilization, Environ. Effects*, pp. 1–20, Mar. 2021, doi: 10.1080/15567036.2021.1895916.

[18] M. N. Nabi, J. E. Hustad, and M. A. Arefin, "The influence of Fischer–Tropsch-biodiesel–diesel blends on energy and exergy parameters in a six-cylinder turbocharged diesel engine," *Energy Rep.*, vol. 6, pp. 832–840, Nov. 2020.

[19] C. Odibi, M. Babaie, A. Zare, M. N. Nabi, T. A. Bodisco, and R. J. Brown, "Exergy analysis of a diesel engine with waste cooking biodiesel and triacetin," *Energy Convers. Manage.*, vol. 198, Oct. 2019, Art. no. 111912.

[20] M. N. Nabi, M. G. Rasul, M. Anwar, and B. J. Mullins, "Energy, exergy, performance, emission and combustion characteristics of diesel engine using new series of non-edible biodiesels," *Renew. Energy*, vol. 140, pp. 647–657, Sep. 2019.

[21] A. Zare, M. N. Nabi, T. A. Bodisco, F. M. Hossain, M. M. Rahman, Z. D. Ristovski, and R. J. Brown, "The effect of triacetin as a fuel additive to waste cooking biodiesel on engine performance and exhaust emissions," *Fuel*, vol. 182, pp. 640–649, Oct. 2016.

[22] M. N. Nabi, M. G. Rasul, and R. J. Brown, "Notable reductions in blow-by and particle emissions during cold and hot start operations from a turbocharged diesel engine using oxygenated fuels," *Fuel Process. Technol.*, vol. 203, Jun. 2020, Art. no. 106394.

[23] H. Chowdhury, T. Chowdhury, M. Thirugnanasambandam, M. Farhan, J. U. Ahamed, R. Saidur, and S. M. Sait, "A study on exergetic efficiency vis-à-vis sustainability of industrial sector in Bangladesh," *J. Cleaner Prod.*, vol. 231, pp. 297–306, Sep. 2019.

[24] G. BoroumandJazi, R. Saidur, B. Rismanchi, and S. Mekhilef, "A review on the relation between the energy and exergy efficiency analysis and the technical characteristic of the renewable energy systems," *Renew. Sustain. Energy Rev.*, vol. 16, no. 5, pp. 3131–3135, Jun. 2012.

[25] M. N. Nabi, A. Zare, F. M. Hossain, M. M. Rahman, T. A. Bodisco, Z. D. Ristovski, and R. J. Brown, "Influence of fuel-borne oxygen on European stationary cycle: Diesel engine performance and emissions with a special emphasis on particulate and NO emissions," *Energy Convers. Manage.*, vol. 127, pp. 187–198, Nov. 2016.

MD. NURUN NABI received the Ph.D. degree from Hokkaido University, Japan. Later, he was a Postdoctoral Researcher at the Norwegian University of Science and Technology, Norway, for two years. He is currently a Senior Lecturer in mechanical engineering at Central Queensland University, Australia. He is also an Internationally Recognized Researcher. He is successful in many multidisciplinary and collaborative research works with industries and universities nationally and internationally. His expertise is to explore sustainable fuels for internal combustion engines, including aviation engines to mitigate emissions to an ultra-low level. So far in his career, he has published more than 141 articles in high impact factor journals, book chapters, and conference proceedings. According to Google Scholar, his current H-index is 35 with over 4613 citations and as per Scopus, the H-index is 28 with over 2898 citations. His current research interest includes decarbonization along with ultra-low emissions using hydrogen fuel. As recognition of his outstanding research contributions, he received a Vice-Chancellor Commendation Award, the Dean's Award, and the Research Recognition Award from Central Queensland University, Australia. One of his SAE technical papers received a Harry L. Horning Memorial Award, which is one of the Outstanding Research Recognition Awards in the emission reduction arena.

WISAM K. HUSSAM is currently an Associate Professor with the Department of Mechanical Engineering, Australian College of Kuwait. His research interests include computational fluid dynamics and heat transfer, hybrid renewable energy systems modeling and optimization, heat transfer enhancement for industrial, and solar energy systems.

MOHAMMAD TOWHIDUL ISLAM has been working as an Active Researcher in the field of thermal engineering, computation fluid dynamics (CFD), hydrogen as fuel, combustion, and emission analysis, since 2017. He is currently working as a Research Assistant with the Department of Mechanical Engineering, Georgia Southern University, Statesboro, GA, USA. Before that, he was worked as a Senior Deputy Assistant Director in compressor research and development at Walton High-Tech Industries Ltd. He is also at Bangladeshi multinational company and has placed 15th in compressor production around the world. It has already covered 38 countries in the world to sell its electrical and electronics products. Before joining this reputed tech-giant, he also worked as an Assistant Engineer in another reputed power generation company based on HFO in Bangladesh. He has completed seven innovative projects among which two projects are fully funded by the University of Grant Commission (UGC) of Bangladesh. He is working on U.S. governmental funded projects related to thermal and fluid dynamics. Besides, he has contributed his research ideas, knowledge and skills in numerous research activities which have been published through some ISI and Scopus indexed journals, proceedings, conferences, and book chapters. His recent book chapter on hydrogen energy titled "Assessment of Hydrogen as an Alternative Fuel: Status, Prospects, Performance and Emission Characteristics" has been published in a book series of *Greener and Scalable E-fuels for Decarbonization of Transport* (Springer Nature, 2022).

S. M. MUYEEN (Senior Member, IEEE) received the B.Sc. degree in engineering from the Rajshahi University of Engineering and Technology (RUET), Bangladesh, formerly known as the Rajshahi Institute of Technology, in 2000, and the M.Eng. and Ph.D. degrees in electrical and electronic engineering from the Kitami Institute of Technology, Japan, in 2005 and 2008, respectively. He is currently working as a Full Professor with the Department of Electrical Engineering, Qatar University. He has published seven books as an author or an editor. He has published more than 300 articles in different journals and international conferences. His research interests include power system stability and control, electrical machine, FACTS, energy storage systems (ESS), renewable energy, and HVDC systems. He is a fellow of Engineers Australia. He is serving as an Editor/Associate Editor for many prestigious journals from IEEE, IET, and other publishers, including IEEE TRANSACTIONS ON ENERGY CONVERSION, IEEE POWER ENGINEERING LETTERS, *IET Renewable Power Generation*, and *IET Generation, Transmission and Distribution*. He has been a keynote speaker and an invited speaker at many international conferences, workshops, and universities.